

**Tropical vegetation
response to Heinrich
Event 1**

D. Handiani et al.

Tropical vegetation response to Heinrich Event 1 as simulated with the UVic ESCM and CCSM3

D. Handiani¹, A. Paul^{1,2}, X. Zhang¹, M. Prange^{1,2}, U. Merkel^{1,2}, and L. Dupont²

¹Department of Geosciences, University of Bremen, Bremen, Germany

²MARUM – Center for Marine Environmental Sciences, University of Bremen, Bremen, Germany

Received: 12 October 2012 – Accepted: 31 October 2012 – Published: 5 November 2012

Correspondence to: D. Handiani (dhandiani@marum.de)

Published by Copernicus Publications on behalf of the European Geosciences Union.

Title Page

Abstract

Introduction

Conclusions

References

Tables

Figures

⏪

⏩

◀

▶

Back

Close

Full Screen / Esc

Printer-friendly Version

Interactive Discussion



Abstract

We investigated changes in tropical climate and vegetation cover associated with abrupt climate change during Heinrich Event 1 (HE1) using two different global climate models: the University of Victoria Earth System-Climate Model (UVic ESCM) and the Community Climate System Model version 3 (CCSM3). Tropical South American and African pollen records suggest that the cooling of the North Atlantic Ocean during HE1 influenced the tropics through a southward shift of the rainbelt. In this study, we simulated the HE1 by applying a freshwater perturbation to the North Atlantic Ocean. The resulting slowdown of the Atlantic Meridional Overturning Circulation was followed by a temperature seesaw between the Northern and Southern Hemispheres, as well as a southward shift of the tropical rainbelt. The shift was more pronounced in the CCSM3 than in the UVic ESCM simulation. Nevertheless, both models suggested a similar response of the vegetation patterns in the tropics around the Atlantic Ocean, where the grass cover increased and the tree cover decreased, specifically in tropical North Africa around 15° N in the UVic ESCM simulation and around 10° N in CCSM3. In the CCSM3 model, the tree and grass cover in tropical Southeast Asia responded to the abrupt climate change during the HE1, which could not be found in the UVic ESCM. The biome distributions derived from both models corroborate findings from pollen records in Southwestern and equatorial Western Africa as well as Northeastern Brazil.

1 Introduction

Heinrich events in general are associated with layers of ice-rafted debris (IRD) in the sediments of the North Atlantic Ocean dated between 70 ka BP (ka BP = thousand years before present) and 14 ka BP (Heinrich, 1988; Broecker, 1994). The Heinrich event 1 (HE1, ca. 17.5 ka BP) is the most recent of these distinctive cold periods in the North Atlantic region. Paleoceanographic evidence suggests a connection between

CPD

8, 5359–5387, 2012

Tropical vegetation response to Heinrich Event 1

D. Handiani et al.

Title Page

Abstract

Introduction

Conclusions

References

Tables

Figures



Back

Close

Full Screen / Esc

Printer-friendly Version

Interactive Discussion



the abrupt climate changes during these events and the variability of the North Atlantic Deep Water (NADW) formation and Atlantic Meridional Overturning Circulation (AMOC, Sarnthein et al., 1994; McManus et al., 2004).

Frequently, a change in the AMOC during the HE1 is invoked to explain an unusual hydrological cycle in the tropics and a southward shift of the Intertropical Convergence Zone (ITCZ) and its associated rainbelt (e.g. Behling et al., 2000). Since vegetation and climate are tightly coupled, tropical climate changes influence the tropical vegetation patterns. This is demonstrated by pollen proxy records, which exhibit changes in the tropics simultaneous with the North Atlantic temperature changes during this event (e.g. Hessler et al., 2010). Some examples are found in Eastern tropical Africa (Kashiru swamp, Burundi), where grassland and dry shrubland occurred due to a fairly cold and dry climate (Bonfille and Riollet, 1988; Hessler et al., 2010) and at Lake Masoko, Tanzania, where warm temperate and mixed forests were formed due to a moderately wet climate (Vincens et al., 2007; Hessler et al., 2010). In tropical South America, pollen records indicate contrasting vegetation changes between the northern and southern limits of the ITCZ (Hessler et al., 2010), e.g. at the Cariaco Basin site (equatorial Northern South America), which had a more open vegetation due to dry climate conditions (González et al., 2008; González and Dupont, 2009), while the Lake Caçó region (equatorial Southern South America) was occupied by a denser forest during the HE1 than in the Last Glacial Maximum (LGM) period due to moist climate conditions (Ledru et al., 2001; Dupont et al., 2009). In Indonesia an open grass-rich vegetation during the LGM was inferred from a marine pollen record (van der Kaars, 1991), although the Borneo rainforest was probably preserved and might have extended to the continental shelf of the South China Sea (Morley, 2000). At the terrestrial Rawa Danau site (West Java, Indonesia), the lowland forest and C3 plant cover increased and the grass cover decreased between 17 to 15.4 ka BP indicating enhanced precipitation (van der Kaars, 2001; Turney et al., 2006).

Previous model studies suggested that the southward shift of the ITCZ occurred as a response to a slowdown of the AMOC during the HE1 (e.g. Stouffer et al., 2006;

Tropical vegetation response to Heinrich Event 1

D. Handiani et al.

Title Page

Abstract

Introduction

Conclusions

References

Tables

Figures



Back

Close

Full Screen / Esc

Printer-friendly Version

Interactive Discussion



Tropical vegetation response to Heinrich Event 1

D. Handiani et al.

Title Page

Abstract

Introduction

Conclusions

References

Tables

Figures



Back

Close

Full Screen / Esc

Printer-friendly Version

Interactive Discussion



Kageyama et al., 2009). In these studies, the AMOC weakening has been induced by perturbing the freshwater balance of the North Atlantic Ocean (e.g. Köhler et al., 2005; Menviel et al., 2008; Kageyama et al., 2010). Using an Earth System Model of Intermediate Complexity (EMIC, Claussen et al., 2002) which includes a dynamic vegetation component, it has been demonstrated that model results and pollen records in tropical Africa and Northern South America are generally consistent (Kageyama et al., 2005; Handiani et al., 2012). However, in many EMICs the atmospheric component is simplified, in particular with respect to the representation of the hydrological cycle. This demands a modeling study using a more complex atmospheric component.

The purpose of our study was to compare the tropical vegetation response to climate changes during the HE1 as simulated by two global climate models that differ in the complexity of their atmospheric components. We employed the University of Victoria Earth System-Climate Model (UVic ESCM, cf. Weaver et al., 2001) and the Community Climate System Model version 3 (CCSM3, Collins et al., 2006; Yeager et al., 2006). Both models contained a dynamic global vegetation component (Meissner et al., 2003; Levis et al., 2004). In addition, the model results were compared to the available pollen records from tropical vegetation. However, the comparison between model results and pollen records is not a straightforward approach. Mostly, a dynamic global vegetation component represents the type of vegetation cover as Plant Functional Types (PFTs), while compilations of pollen records are available in terms of biome distributions (Prentice et al., 1996; Hessler et al., 2010). To allow comparison between models and pollen records directly, either the pollen records are assigned to PFTs or the model results are converted into biome distributions. In our study, the simulated vegetation covers were mapped onto biome distributions (Schurgers et al., 2006; Handiani et al., 2012) allowing for both a model intercomparison and a comparison of the simulated biogeographies to pollen-based reconstructions.

2 Models and experimental design

In the present study, we used the UVic ESCM version 2.8 (Weaver et al., 2001). The atmospheric component of this model contains a parameterization of anomalous near-surface winds to take into account the dynamical wind feedback (Fanning and Weaver, 1997). Furthermore, the dynamic vegetation model TRIFFID (Cox, 2001) is included in this version of the UVic ESCM to simulate the terrestrial biosphere in terms of soil carbon storage and five PFTs (Table 1). All components of the UVic ESCM share the same resolution of 3.6° by 1.8° (longitude × latitude) with one vertically-averaged layer in the atmospheric model and nineteen vertical levels in the ocean model.

In addition, we made use of the state-of-the-art coupled general circulation model CCSM3 (Collins et al., 2006). Here, we employed the low-resolution version of CCSM3 which is described in detail by Yeager et al. (2006). In this version, the resolution of the atmosphere is given by T31 (3.75° transform grid) spectral truncation with 26 layers, while the ocean model has a nominal horizontal resolution of 3° (like the sea-ice component) with 25 levels in the vertical. The latitudinal resolution of the ocean grid is variable, with finer resolution around the equator (0.9°).

The dynamic global vegetation model (DGVM; Levis et al., 2004) is based on the Lund-Potsdam-Jena (LPJ) model (Sitch et al., 2003; Bonan and Levis, 2006). It is coupled to the Community Land Model version 3 (CLM3; Oleson et al., 2004), and thus we refer to it as the CLM-DGVM. CLM-DGVM has the same horizontal resolution as the atmosphere. In order to improve the simulation of land surface hydrology, which affects the biogeography of vegetation, we implemented new parameterizations for canopy interception and soil evaporation into the CLM-DGVM following Oleson et al. (2008). The model simulates ten PFTs, which differ in their physiological, morphological, phenological, bioclimatic and fire-response attributes. Seven PFTs refer to trees and three PFTs to non-tree vegetation cover (Table 1).

Tropical vegetation response to Heinrich Event 1

D. Handiani et al.

Title Page

Abstract

Introduction

Conclusions

References

Tables

Figures



Back

Close

Full Screen / Esc

Printer-friendly Version

Interactive Discussion



We performed two sets of experiments with each model. Each set of experiments was meant to simulate the vegetation distribution characteristic of the background climate of the LGM and HE1. The experimental design is summarized below:

1. The LGM simulations were forced by the boundary conditions of 21 ka BP. The LGM simulation with the UVic ESCM (LGM_UVic) was similar to the LGM simulation by Handiani et al. (2012). The LGM simulation with the CCSM3 (LGM_CCSM) was similar to the CCSM3 LGM simulation by Merkel et al. (2010), except that the DGVM was activated and the land surface hydrology was improved (see above). Both LGM simulations were integrated until equilibrium was reached, which was taken to be after 2000 yr for the LGM_UVic and 1500 yr for the LGM_CCSM simulation.
2. The HE1 simulations were identical to the LGM simulations as described in (1), except that a freshwater flux anomaly was imposed on the North Atlantic Ocean, which was added in both models at the same constant rate of 0.2 Sv ($1 \text{ Sv} = 10^6 \text{ m}^3 \text{ s}^{-1}$) for the whole duration of the experiment (500 model years). The location of the freshwater flux anomaly is described in Handiani et al. (2012) for the HE1_UVic and in Merkel et al. (2010) for the HE1_CCSM simulation.

In contrast to the UVic simulations by Handiani et al. (2012), the UVic ESCM simulations used here included a parameterization of the dynamic wind feedback. In the parameterization, wind field and wind stress anomalies are calculated from surface air temperature anomalies (Weaver et al., 2001). These wind field and wind stress anomalies are then added to the prescribed mean wind field in order to account for the dynamic response of the atmosphere to sea surface temperature anomalies, which has a stabilizing effect on the AMOC (Fanning and Weaver, 1997).

The model analysis and discussion refer to model output time-averaged over the last 100 yr of each simulation. As specified above, the two models simulate a different number of PFTs. Therefore, to facilitate model comparison, the PFT output of each model was classified into four generic types of PFTs, namely broadleaf evergreen trees,

Tropical vegetation response to Heinrich Event 1

D. Handiani et al.

Title Page

Abstract

Introduction

Conclusions

References

Tables

Figures



Back

Close

Full Screen / Esc

Printer-friendly Version

Interactive Discussion



needleleaf evergreen trees, deciduous trees and grasses (see Table 1). The PFT cover and the surface temperature of each model were used to generate the biome distribution. Given the different number of simulated PFTs, a different scheme to estimate the biome distribution had to be used for each model. The scheme for the UVic ESCM (Table 2) is described by Handiani et al. (2012) and uses the fractional coverage of the five PFTs and the atmospheric temperature from the model output. The percentage of PFT coverage allowed to evaluate the dominant PFT in each grid cell of the model (Table 2a). The simulated atmospheric temperatures served to calculate the environmental constraints for the biomes, such as temperature of the coldest month (T_c), temperature of the warmest month (T_w), and the number of growing degree-days above 0 and 5 °C (GDD0 and GDD5, respectively, Table 2b). The scheme for the CCSM3 was adopted from a study by Schurgers et al. (2006), who applied it to the LPJ model output for the Eemian and the Holocene (Table 3). It was used applied to the fractional coverage of the ten PFTs (Table 1) from the output of the CLM-DGVM model, together with the air surface temperature from the atmospheric model. These biomes (1) can be derived from the UVic ESCM and the CCSM3 output without degenerating into arbitrariness and still show shifts of vegetation cover in simulations of long time scales and (2) allow for a direct comparison to the vegetation cover reconstructed from the pollen records.

3 Results

3.1 Climate changes

The AMOC gradually decreased in both models in response to the freshwater perturbation, but in each model the degree of reduction was different (not shown). In the LGM_UVic simulation, the maximum of the AMOC streamfunction started from a maximum strength of ~12 Sv, and eventually collapsed after 100 yr simulation time, while in the LGM_CCSM simulation, it decreased from 14 Sv to 4 Sv. This weakened or even collapsed AMOC was in both models accompanied by a strong cooling in the Northern

Tropical vegetation response to Heinrich Event 1

D. Handiani et al.

Title Page

Abstract

Introduction

Conclusions

References

Tables

Figures



Back

Close

Full Screen / Esc

Printer-friendly Version

Interactive Discussion



Hemisphere and a slight warming in the Southern Hemisphere (Fig. 1a, c). The cooling is most pronounced in the surface air temperature decrease over the North Atlantic Ocean. However, the regional pattern and amplitude of the surface air temperature anomaly is very different between the two models. The negative surface temperature anomalies for HE1 were around -2°C for the UVic ESCM and around -4°C for the CCSM3 off Northwest Africa. The positive temperature anomalies in the Southern Hemisphere were also larger in the CCSM3 than in the UVic ESCM. In the tropics, the climate simulated by the UVic ESCM was only slightly (between 0 to 1°C) colder in the HE1 experiment compared to the LGM experiment, whereas in the CCSM3, the northern equatorial Atlantic Ocean was colder by up to 2°C (Fig. 1c).

The weakening of the AMOC and an asymmetric surface temperature response between the two hemispheres were responsible for a southward shift of the tropical rainbelt as suggested by the simulated precipitation patterns (Fig. 1b, d). The pattern in the UVic ESCM was of rather large scale and extended beyond the ITCZ region. In the tropical Atlantic region, the precipitation differences between the HE1_UVic and the LGM_UVic simulation were around -0.25mm day^{-1} north of the equator and 0.5mm day^{-1} south of the equator (Fig. 1b). In the CCSM3, the precipitation differences between the HE1 and the LGM simulation were around -2.5mm day^{-1} north of the equator and 2.0mm day^{-1} south of the equator (Fig. 1c). The precipitation differences for CCSM3 were much larger between 10°S and 10°N in the tropics than in the other regions. The anomalies of the zonally averaged precipitation in CCSM3 showed a drying north of the equator by up to 0.8mm day^{-1} and a wetting south of the equator by a similar amount, thus sharply reflecting the southward shift of the rainbelt (Fig. 1e). A comparison of the magnitude of precipitation anomalies in the HE1_UVic and the HE1_CCSM simulations revealed that the minimum and maximum anomalies in the HE1_UVic simulation were clearly weaker (min. -0.86mm day^{-1} and max. of 0.48mm day^{-1}) compared to the HE1_CCSM simulation (min. of -4.19mm day^{-1} and max. of 2.80mm day^{-1}).

Tropical vegetation response to Heinrich Event 1

D. Handiani et al.

[Title Page](#)[Abstract](#)[Introduction](#)[Conclusions](#)[References](#)[Tables](#)[Figures](#)[Back](#)[Close](#)[Full Screen / Esc](#)[Printer-friendly Version](#)[Interactive Discussion](#)

3.2 The vegetation cover response

In this section, we will discuss changes in vegetation cover in terms of the simplified PFTs as defined in Table 1 (see also Sect. 2), which allows for a direct comparison between the output from the UVic ESCM and the CCSM3. Our results showed that the southward shift of the tropical rainbelt triggered vegetation changes in the tropics, with spatially varying degree and dominance. In both HE1 experiments, broadleaf evergreen trees cover decreased in equatorial Northern Africa (Fig. 2a, b). In the UVic ESCM, it was reduced by 60 % in the Sahel region and Southeastern Brazil and between 20 % to 40 % in equatorial Western South America (Fig. 2a). The pattern was similar in CCSM3, specifically in equatorial Africa region, except that the change amounted to 40 % (Fig. 2b). Moreover, in CCSM3 the broadleaf evergreen tree cover also decreased in Southeast Brazil and by 40 % in a small region on the west coast of Africa, and it increased with similar percentages in equatorial Western South America. Furthermore, the decrease in broadleaf tree cover in Southeast Asia was less than 10 % in the UVic ESCM but around 20 % in the CCSM3 (Fig. 2a, b).

In the tropics, the needleleaf evergreen tree cover was relatively unaffected in both HE1 experiments, except for a small decrease in Eastern Brazil and the Central Sahel region in the UVic ESCM and in Southwest South America in the CCSM3 simulation (Fig. 2c, d). However, the deciduous tree cover was reduced by more than 60 % in the Eastern Sahel region in the UVic ESCM and by a similar percentage in equatorial Western South America, the Central Sahel region and Southeast Asia in the CCSM3 (Fig. 2e, f). In contrast, the deciduous tree cover in Central Brazil increased by around 60 % in both models. Meanwhile, in tropical Northern Africa (i.e. the Sahel region), the grass cover increased by around 60 % in both models. However, with the UVic ESCM result located the grass cover further north and has over a wider longitude ranges than compare to the CCSM3. In tropical South America, the grass cover was relatively unchanged in the UVic ESCM simulation, while it mostly decreased in the CCSM3 simulation (Fig. 2g, h). The grass cover change was more pronounced in the

Tropical vegetation response to Heinrich Event 1

D. Handiani et al.

Title Page

Abstract

Introduction

Conclusions

References

Tables

Figures



Back

Close

Full Screen / Esc

Printer-friendly Version

Interactive Discussion



CCSM3 simulation than in the UVic ESCM simulation, e.g. it was reduced in tropical North America and South America, while it increased by 20 to 40 % in Northwest South America and tropical Africa and by about 60 % in Southeast Asia (Fig. 2h). It was reduced by 20 to 80 % in tropical Western Africa, while it increased by up to 80 % in tropical Central and Eastern Africa (Fig. 2g).

The annual-mean anomalies of the zonally averaged tree and grass cover between the HE1 and the LGM experiments reflected the PFT differences in tropical locations of South America (Fig. 3a, b), Africa (Fig. 3c, d) and Southeast Asia (Fig. 3e, f). In some locations equal but opposite vegetation changes occurred, e.g. the tree cover in the UVic ESCM was reduced by 60 % in tropical Africa around 15° N, while the grass cover increased by a similar percentage at the same latitude (Fig. 3c). A similar pattern also emerged from the CCSM3 simulation, where at around 10° N the tree cover decreased by 20 % while the grass cover increased by a similar percentage (Fig. 3d). Moreover, in tropical South America, the tree and the grass cover in the CCSM3 simulation were reduced by about 30–50 % between 5° N–10° N, while an opposite change of tree and grass cover by about 10–30 % occurred around 10° S (Fig. 3b). The tree and grass cover in the UVic ESCM south of the equator (~ 15° S) discussed so far (Fig. 3a, c, e) showed differences of less than 5 %, whereas the differences in CCSM3 (Fig. 3b, d, f) are at least larger than 10 %. While the UVic ESCM did not show any pronounced changes in tropical Southeast Asia (Fig. 3e), the CCSM3 tree cover generally decreased and the grass cover increased in that region (Fig. 3f).

3.3 Biome distribution comparison

In this section, we compare our model results to data. For this comparison, we used pollen records for HE1 from tropical South America and tropical Africa (Fig. 4a) compiled by Hessler et al. (2010). In Fig. 4, a comparison is presented to show where model results are consistent with proxy information. The changes in tropical African forest as found in the HE1_UVic and the HE1_CCSM simulations mostly agreed with the pollen reconstruction (Fig. 4b, c). According to both models and the pollen records, equatorial

Tropical vegetation response to Heinrich Event 1

D. Handiani et al.

Title Page

Abstract

Introduction

Conclusions

References

Tables

Figures



Back

Close

Full Screen / Esc

Printer-friendly Version

Interactive Discussion



Tropical vegetation response to Heinrich Event 1

D. Handiani et al.

Title Page

Abstract

Introduction

Conclusions

References

Tables

Figures



Back

Close

Full Screen / Esc

Printer-friendly Version

Interactive Discussion



Western Africa was covered by tropical forest corresponding to a wet climate. In Southwest Africa, the pollen records indicated a warm temperate forest and farther south savannah (Fig. 4a). The HE1_UVic simulation agreed with both records in Southwest Africa, while the HE1_CCSM simulation only agreed with one record (Fig. 4a, b) because the HE1_CCSM predicted savannah due to a relatively warm climate in these locations (Fig. 4c). Another discrepancy between the HE1_CCSM simulation and the pollen records is found in Eastern Africa, where the model predicted tropical forest and grassland, while the records suggest warm-temperate forest and savannah (Fig. 4c).

The biome distributions derived from the model and pollen results were in disagreement at the Colônia site (Brazil). According to the pollen record, savannah covered this region indicating a warm and dry climate (Fig. 4). The tropical forest in the HE1_UVic and the HE1_CCSM simulations was broadly consistent with the pollen records of Lake Caçó (Northeast Brazil). The HE1_CCSM simulations was also in agreement with the pollen record of core GeoB 3910-2 off the coast of Northeast Brazil (site number 10 in Fig. 4a); both model and data indicated savannah (Fig. 4c). In contrast, for the same region, the HE1_UVic simulation predicted tropical forest (Fig. 4b).

A tropical Asian biome reconstruction for HE1 is not available yet; hence it is difficult to perform a thorough model-data comparison. However, the simulation of a savannah corridor in Sundaland in CCSM3 is worth noting as the existence of such a feature during the last glaciation is highly debated (e.g. Bird et al., 2005). From a modeling perspective, the changes in the biome distributions between the HE1 and LGM simulations were insignificant (not shown, but see the PFT cover anomalies), although some changes did occur in the CCSM3 model. For example, grass cover increased in southeast China and replaced savannah in the HE1_CCSM simulation (Fig. 4c).

4 Discussion

The simulations in the UVic ESCM presented here are different from Handiani et al. (2012). Both studies used the UVic ESCM and an identical experimental design,

however, Handiani et al. (2012) did not include the dynamical wind feedback parameterization. Regarding the precipitation patterns in the tropics, there are a few differences between the earlier study by Handiani et al. (2012) and our present study. Our preindustrial simulation (not shown) resulted in a climate that was warmer and drier than in the study by Handiani et al. (2012), most notably in equatorial Southern South America and Africa as well as the Sahel region. Nevertheless, the HE1 simulations of both studies suggested similar tropical precipitation anomalies. Thus including the dynamical wind feedback parameterization in the UVic ESCM improved the representation of the precipitation pattern in the ITCZ region in the preindustrial simulation (not shown), but it only had a slight impact on the tropical precipitation response in the HE1 simulation. Moreover, despite the additional moisture transport by advection in this version of the UVic ESCM, the precipitation in the terrestrial tropics and the ITCZ region was still weaker as compared to the CCSM3. Weaver et al. (2001), who introduce the moisture transport by advection in the UVic ESCM, identify additional regions such as the mid-latitude North Atlantic Ocean and Pacific Ocean regions that need further improvement. The inclusion of dynamical wind feedback parameterization in the atmospheric model in this version of the UVic ESCM barely influences the tropical vegetation cover distribution in the preindustrial simulation (not shown). The comparison between Handiani et al. (2012) and this study (not shown) shows a great similarity of preindustrial tropical vegetation cover. The smooth precipitation distribution from both preindustrial simulations led to a similar smooth vegetation distribution in the tropics. For example, tree cover penetrated into the subtropics of Northern and Southern Africa (not shown, see Handiani et al., 2012).

The slowdown of the AMOC during the HE1 simulation caused an adjustment of the surface temperature called the “bipolar seesaw”, which is characterized by a cooling in the Northern Hemisphere and a slight warming in the Southern Hemisphere (Broecker et al., 1985). In the tropics, the bipolar seesaw in turn influenced the precipitation patterns. Positive anomalies developed over the equatorial South Atlantic Ocean and surrounding regions, while negative anomalies appeared over the tropical North

Tropical vegetation response to Heinrich Event 1

D. Handiani et al.

Title Page

Abstract

Introduction

Conclusions

References

Tables

Figures



Back

Close

Full Screen / Esc

Printer-friendly Version

Interactive Discussion



Tropical vegetation response to Heinrich Event 1

D. Handiani et al.

Title Page

Abstract

Introduction

Conclusions

References

Tables

Figures



Back

Close

Full Screen / Esc

Printer-friendly Version

Interactive Discussion



Atlantic Ocean. In the CCSM3, the positive anomaly spanned an entire band south of the equator from Central Brazil to Central Africa with the maximum of this band over Eastern Brazil. The negative anomalies ranged from the Sahel to Central America. These anomalies also occurred in the UVic ESCM, although much less pronounced as compared to the CCSM3. In the UVic ESCM, the highest positive anomalies extended farther into southeast South America and Western Angola, while maximum negative anomalies were found in the Sahel region.

Pronounced changes in broadleaf tree cover in the tropics were confined to the Sahel region, equatorial Southern South America and Western Africa. This suggests that these regions were most sensitive to a shift of the tropical rainbelt in response to a slow-down of the AMOC. Changes in tree cover were related to changes in grass cover. We indeed expected a shift from tropical trees to grass cover due to a drier climate in the Sahel region and a shift from grass cover to tree cover due to a wetter climate in equatorial Southern South America. This was confirmed by the HE1_CCSM results around 10° S in tropical South America and around 10° N in tropical Africa, where tree cover and grass cover changed by comparable magnitudes. Similarly, according to the HE1_UVic results around 15° N in tropical Africa, tree cover decreased significantly while grass cover increased. Such a pattern is also found in the HE1 experiments by Scholze et al. (2003), Köhler et al. (2005) and Menviel et al. (2008), where the vegetation shifts occur in the latitudinal band between 5° S and 15° N.

According to Bonan and Levis (2006), the tropical forest in South America under present climate conditions is less extensive in CCSM3 than in the observations. The complex interaction within the hydrological cycle (between soil moisture, vegetation, evaporation, transpiration and precipitation) in that region leads to a considerable decrease in precipitation and tree cover. As a consequence, the broadleaf tree cover in tropical South America under preindustrial climate conditions was smaller in the CCSM3 than in the UVic ESCM. Similarly, in the HE1_CCSM simulation, tropical South America was covered by more open vegetation (e.g. savannah and grassland) than in the HE1_UVic simulation. However, the biome distribution in the HE1_CCSM simulation

proved to be in agreement with pollen sites in tropical South America, and in spite of the deficiency of the simulated hydrological cycle in tropical South America, the CCSM3 captured the climate change in western tropical Africa during HE1 quite well.

The tropical forest simulated by both models in Southeast Asia is supported by Morley (2000), who suggests that the Borneo tropical forest persisted and even extended onto the continental shelf of the South China Sea during the last glacial period. Nevertheless, CCSM3 also suggested the appearance of a savannah corridor in Sundaland as it has first been proposed by Heaney (1991). Moreover, in the HE1_CCSM simulation, the vegetation cover in tropical Southeast Asia responded to abrupt climate change in the Northern Atlantic Ocean with changes in tree and grass cover of around 20%. These changes were significantly larger than in the HE1_UVic simulation, which were less than 10%. The CCSM3 results can be considered as an indication of a teleconnection between North Atlantic Ocean climate and vegetation cover in tropical Southeast Asia (e.g. Zhou et al., 2007; Lee et al., 2011). However, a more extensive compilation of paleovegetation data from this region is needed to ease the comparison between model and data and to corroborate this finding.

Comparing model output and pollen records is not an easy task; one example from our study is that the definitions of the PFTs are not exactly the same. This problem becomes apparent when comparing pollen reconstructions from specific geographic locations (e.g. a mountain or lake) with model results, which often cannot represent those locations in the required detail. Since models are mostly formulated in terms of PFTs, but are checked for consistency against pollen records or the present-day vegetation distribution, either the PFTs from the model output have to be converted into a biome distribution, or the biome distribution from the pollen records has to be converted into PFTs. Several model studies have tackled this situation by developing a scheme to compute biomes based on the PFTs from the model output (e.g. Crucifix et al., 2005; Roche et al., 2007; Schurgers et al., 2006; Handiani et al., 2012). The weakness of this approach is that the calculation depends on specific model output; hence a scheme for one model can not be used directly for another model. This was suggested in our two

Tropical vegetation response to Heinrich Event 1

D. Handiani et al.

Title Page

Abstract

Introduction

Conclusions

References

Tables

Figures



Back

Close

Full Screen / Esc

Printer-friendly Version

Interactive Discussion



schemes for the UVic ESCM and the CCSM3. In contrast, a number of techniques have been developed to convert the biome distribution derived from satellite or observational data into PFTs (e.g. Meissner et al., 2003; Poulter et al., 2011). Unfortunately, these approaches can only be used for present-day model results, since biome distributions derived from satellite data is only available for the present-day vegetation.

5 Conclusions

This study compared two simulations of HE1 by two different earth system models. Both models simulated a slowdown of the AMOC in response to a freshwater perturbation in the North Atlantic Ocean. The associated bipolar seesaw in surface temperature influenced the tropical climate through a southward shift of the rainbelt. However, the effect on precipitation was smaller in the UVic ESCM than in the CCSM3.

The shift of the tropical rainbelt caused drier climate conditions in the northern equatorial region and wetter climate conditions in the southern equatorial region, which also influenced the tropical vegetation patterns, specifically in tropical Africa around 15° N in the UVic ESCM and 10° N in the CCSM3. In southern equatorial Africa, there was no visible response to the freshwater hosing in the UVic ESCM, while in the CCSM3 opposite tree and grass cover changes occurred around 15° S. The tree and grass cover in the CCSM3 in tropical South America also suggested opposite changes south of the equator (10° S), while north of the equator (between 5° N and 10° N) both decreased due to a drier climate. In addition, tree cover decreased and grass cover increased between 10° N and 15° N, and between 0 and 10° S in Southeast Asia during the HE1 experiment in CCSM3.

The direct comparison of the simulated biome distribution and pollen records provides for an assessment of the model-data agreement without relying on indirect reconstructions of precipitation and temperature distributions from pollen records. Nevertheless, comparing model and pollen records has its own uncertainties; one of it is to have a coherent classification of biome distribution for both model and pollen records.

Tropical vegetation response to Heinrich Event 1

D. Handiani et al.

Title Page

Abstract

Introduction

Conclusions

References

Tables

Figures



Back

Close

Full Screen / Esc

Printer-friendly Version

Interactive Discussion



For our study, we applied two such biomisation schemes, specific to each model, which allowed for a comparison between the model results and the available pollen records.

Finally, the agreement with the reconstructed biome distribution during HE1 varied in each model. The best correspondence was found in Southwestern and equatorial Western Africa as well as in Northeastern Brazil. The vegetation cover simulated by CCSM3 in tropical Southeast Asia opens up the possibility that abrupt climate change in the North Atlantic Ocean may have a large-scale, even global impact on the terrestrial biosphere.

Acknowledgements. This work was funded by the Deutsche Forschungsgemeinschaft (DFG) as part of the German contribution to the Integrated Ocean Drilling Program (SPP 527) “Abrupt Climate Change in the African Tropics (ACCAT)” and the DFG Research Center/Excellence Cluster “The Ocean in the Earth System”. The CCSM3 climate model experiments were run on the SGI Altix Supercomputer of the “Norddeutscher Verbund für Hoch- und Höchstleistungsrechnen” (HLRN). The authors are grateful to the Climate Modelling Group at the University of Victoria for providing the UVic ESCM.

References

- Behling, H., Arz, H. W., Pätzold, J., and Wefer, G.: Late Quaternary vegetational and climate dynamics in Northeastern Brazil, inferences from marine core GeoB 3104-1, *Quaternary Sci. Rev.*, 19, 981–994, 2000.
- Bird, M. I., Taylor, D., and Hunt, C.: Paleoenvironment of insular Southeast Asia during the last glacial period: a savanna corridor in Sundaland?, *Quaternary Sci. Rev.*, 24, 2228–2242, 2005.
- Bonan, G. B. and Levis, S.: Evaluating aspects of the community land and atmosphere models (CLM3 and CAM3) using a dynamic global vegetation model, *J. Climate*, 19, 2290–2301, 2006.
- Bonan, G. B., Levis, S., Sitch, S., Vertenstein, M., and Oleson, K. W.: A dynamic global vegetation model for use with climate models: concepts and description of simulated vegetation dynamics, *Global Change Biol.*, 9, 1543–1566, 2003.

Tropical vegetation response to Heinrich Event 1

D. Handiani et al.

Title Page

Abstract

Introduction

Conclusions

References

Tables

Figures



Back

Close

Full Screen / Esc

Printer-friendly Version

Interactive Discussion



Tropical vegetation response to Heinrich Event 1

D. Handiani et al.

Title Page

Abstract

Introduction

Conclusions

References

Tables

Figures



Back

Close

Full Screen / Esc

Printer-friendly Version

Interactive Discussion



- Bonnefille, R. and Riollet, G.: The Kashiru pollen sequence (Burundi), palaeoclimatic implications for the last 40,000 yr. B. P. in tropical Africa, *Quaternary Res.*, 30, 19–35, 1988.
- Broecker, W. S.: Massive iceberg discharges as triggers for global climate change, *Nature*, 372, 421–424, 1994.
- 5 Broecker, W. S., Peteet, D. M., and Rind, D.: Does the ocean-atmosphere system have more than one stable mode of operation?, *Nature*, 315, 21–26, 1985.
- Claussen, M., Mysak, L. A., Weaver, A. J., Crucifix, M., Fichet, T., Loutre, M. F., Weber, S. L., Alcamo, J., Alexeev, V. A., Berger, A., Calov, R., Ganopolski, A., Goosse, H., Lohmann, G., Lunkeit, F., Mokhov, I., Petoukhov, V., Stone, P., and Wang, Z.: Earth system models of intermediate complexity: closing the gap in the spectrum of climate system models, *Clim. Dynam.*, 18, 579–586, 2002.
- 10 Collins, W. D., Rasch, P. J., Boville, B. A., Hack, J. J., McCaa, J. R., Williamson, D. L., Briegleb B. P., Bitz, C. M., Lin, S.-J., and Zhang, M.: The formulation and atmospheric simulation of the Community Atmosphere Model version 3 (CAM3), *J. Climate*, 19, 2144–2161, 2006.
- 15 Cox, P. M.: Description of the “TRIFFID” dynamic global vegetation model, Hadley Centre Technical Note 24, Met Office, Bracknell, 2001.
- Crucifix, M., Betts, R. A., and Hewitt, C. D.: Pre-industrial potential and Last Glacial Maximum global vegetation simulated with a coupled climate-biosphere model: diagnosis of bioclimatic relationships, *Global Planet. Change*, 45, 295–312, 2005.
- 20 Dupont, L. M., Schlütz, F., Teboh Ewah, C., Jennerjahn, T. C., Paul, A., and Behling, H.: Two-step vegetation response to enhanced precipitation in Northeast Brazil during Heinrich event 1, *Global Change Biol.*, 16, 1647–1660, 2009.
- Fanning, A. G. and Weaver, A. J.: On the role of flux adjustments in an idealized coupled climate model, *Clim. Dynam.*, 13, 691–701, 1997.
- 25 González, C. and Dupont, L. M.: Tropical salt marsh succession as sea-level indicator during Heinrich events, *Quaternary Sci. Rev.*, 28, 939–946, 2009.
- González, C., Dupont, L. M., Behling, H., and Wefer, G.: Neotropical vegetation response to rapid climate changes during the last glacial period: palynological evidence from the Cariaco Basin, *Quaternary Res.*, 69, 217–230, 2008.
- 30 Handiani, D., Paul, A., and Dupont, L.: Tropical climate and vegetation changes during Heinrich Event 1: a model-data comparison, *Clim. Past*, 8, 37–57, doi:10.5194/cp-8-37-2012, 2012.

Tropical vegetation response to Heinrich Event 1

D. Handiani et al.

Title Page

Abstract

Introduction

Conclusions

References

Tables

Figures

◀

▶

◀

▶

Back

Close

Full Screen / Esc

Printer-friendly Version

Interactive Discussion



- Harrison, S. P., Yu, G., Takahara, H., and Prentice, I. C.: Palaeovegetation – diversity of temperate plants in East Asia, *Nature*, 413, 129–130, 2001.
- Heaney, L. R.: A synopsis of climatic and vegetational change in Southeast Asia, *Climatic Change*, 19, 53–61, doi:10.1007/BF00142213, 1991.
- 5 Heinrich, H.: Origin and consequences of cyclic ice rafting in the Northeast Atlantic Ocean during the past 130,000 years, *Quaternary Res.*, 29, 142–152, 1988.
- Hessler, I., Dupont, L. M., Bonnefille, R., Behling, H., González, C., Helmens, K. F., Hooghiemstra, H., Lebamba, J., Ledru, M.-P., Lézine, A.-M., Maley, J., Marret, F., and Vincens, A.: Millennial-scale changes in vegetation records from tropical Africa and South America during the last glacial, *Quaternary Sci. Rev.*, 29, 2882–2899, doi:10.1016/j.quascirev.2009.11.029, 2010.
- 10 Kageyama, M., Combourieu Nebout, N., Sepulchre, P., Peyron, O., Krinner, G., Ramstein, G., and Cazet, J.-P.: The Last Glacial Maximum and Heinrich Event 1 in terms of climate and vegetation around the Alboran Sea: a preliminary model-data comparison, *C. R. Geosci.*, 337, 983–992, 2005.
- 15 Kageyama, M., Mignot, J., Swingedouw, D., Marzin, C., Alkama, R., and Marti, O.: Glacial climate sensitivity to different states of the Atlantic Meridional Overturning Circulation: results from the IPSL model, *Clim. Past*, 5, 551–570, doi:10.5194/cp-5-551-2009, 2009.
- Kageyama, M., Paul, A., Roche, D. M., and Van Meerbeeck, C. J.: Modelling glacial climatic millennial-scale variability related to changes in the Atlantic meridional overturning circulation: a review, *Quaternary Sci. Rev.*, 29, 2931–2956, 2010.
- 20 Kaplan, J. O., Bigelow, N. H., Bartlein, P. J., Christensen, T. R., Cramer, W., Harrison, S. P., Matveyeva, N. V., McGuire, A. D., Murray, D. F., Prentice, I. C., Razzhivin, V. Y., Smith, B., Walker, D. A., Anderson, P. M., Andreev, A. A., Brubaker, L. B., Edwards, M. E., Lozhkin, A. V., and Ritchie, J.: Climate change and Arctic ecosystems II: modeling, palaeodatamodel comparisons, and future projections, *J. Geophys. Res.*, 108, 8171, doi:10.1029/2002JD002559, 2003.
- 25 Köhler, P., Joos, F., Gerber, S., and Knutti, R.: Simulated changes in vegetation distribution, land carbon storage, and atmospheric CO₂ in response to a collapse of the North Atlantic thermohaline circulation, *Clim. Dynam.*, 25, 689–708, 2005.
- Ledru, M.-P., Campello, R. C., Landim-Dominguez, J. M., Martin, L., Mourguirat, P., Sifeddine, A., and Turcq, B.: Late-Glacial cooling in Amazonia inferred from pollen at Lagoa do Caçó, Northern Brazil, *Quaternary Res.*, 55, 47–56, 2001.

Tropical vegetation response to Heinrich Event 1

D. Handiani et al.

Title Page

Abstract

Introduction

Conclusions

References

Tables

Figures

◀

▶

◀

▶

Back

Close

Full Screen / Esc

Printer-friendly Version

Interactive Discussion



- Lee, S.-Y., Chiang, J. C. H., Matsumoto, K., and Tokos, K. S.: Southern Ocean wind response to North Atlantic cooling and the rise in atmospheric CO₂: modeling perspective and paleoceanographic implications, *Paleoceanography*, 26, PA1214, doi:10.1029/2010PA002004, 2011.
- 5 McManus, J. F., François, R., Gherardi, J.-M., Keigwin, L. D., and Brown-Leger, S.: Collapse and rapid resumption of Atlantic meridional circulation linked to deglacial climate changes, *Nature*, 428, 834–837, 2004.
- Meissner, K. J., Weaver, A. J., Matthews, H. D., and Cox, P. M.: The role of land surface dynamics in glacial inception: a study with the UVic Earth system model, *Clim. Dynam.*, 21, 515–537, 2003.
- 10 Menviel, L., Timmermann, A., Mouchet, A., and Timm, O.: Meridional reorganizations of marine and terrestrial productivity during Heinrich events, *Paleoceanography*, 23, PA1203, doi:10.1029/2007PA001445, 2008.
- Merkel, U., Prange, M., and Schulz, M.: ENSO variability and teleconnections during glacial climates, *Quaternary Sci. Rev.*, 29, 86–100, 2010.
- 15 Morley, R. J.: *Origin and Evolution of Tropical Forests*, Wiley, Chichester, 2000.
- Oleson, K. W., Lawrence, D. M., Bonan, G. B., Flanner, M. G., Kluzek, E., Lawrence, P. J., Levis, S., Swenson, S. C., Thornton, P. E., Dai, A., Decker, M., Dickinson, R., Feddema, J., Heald, C. L., Hoffman, F., Lamarque, J.-F., Mahowald, N., Niu, G.-Y., Qian, T., Randerson, J., Running, S., Sakaguchi, K., Slater, A., Stöckli, R., Wang, A., Yang, Z.-L., Zeng, X., and Zeng, X.: Technical description of the Community Land Model (CLM), NCAR Tech. Note TN-461+STR, 173, National Center of Atmospheric Research, Boulder, Colorado, 2004.
- 20 Oleson, K. W., Niu, G.-Y., Yang, Z.-L., Lawrence, D. M., Thornton, P. E., Lawrence, P. J., Stockli, R., Dickinson, R. E., Bonan, G. B., Levis, S., Dai, A., and Qian, T.: Improvements to the community land model and their impact on the hydrological cycle, *J. Geophys. Res.*, 25, 113, G01021, doi:10.1029/2007JG000563, 2008.
- Poulter, B., Ciais, P., Hodson, E., Lischke, H., Maignan, F., Plummer, S., and Zimmermann, N. E.: Plant functional type mapping for earth system models, *Geosci. Model Dev.*, 4, 993–1010, doi:10.5194/gmd-4-993-2011, 2011.
- 30 Prentice, J. C., Guiot, J., Huntley, B., Jolly, D., and Cheddadi, R.: Reconstructing biomes from palaeoecological data: a general method and its application to European pollen data at 0 and 6 ka, *Clim. Dynam.*, 12, 185–194, 1996.

Tropical vegetation response to Heinrich Event 1

D. Handiani et al.

[Title Page](#)
[Abstract](#)
[Introduction](#)
[Conclusions](#)
[References](#)
[Tables](#)
[Figures](#)
[Back](#)
[Close](#)
[Full Screen / Esc](#)
[Printer-friendly Version](#)
[Interactive Discussion](#)


Roche, D. M., Dokken, T. M., Goosse, H., Renssen, H., and Weber, S. L.: Climate of the Last Glacial Maximum: sensitivity studies and model-data comparison with the LOVECLIM coupled model, *Clim. Past*, 3, 205–224, doi:10.5194/cp-3-205-2007, 2007.

Sarnthein, M., Winn, K., Jung, S. J. A., Duplessy, J. C., Labeyrie, L., Erlenkeuser, H., and Ganssen, G.: Changes in East Atlantic deep water circulation over the last 30,000 years: an eight time-slice record, *Paleoceanography*, 9, 209–267, 1994.

Scholze, M., Knorr, W., and Heimann, M.: Modelling terrestrial vegetation dynamics and carbon cycling for an abrupt climatic change event, *Holocene*, 13, 327–333, 2003.

Schurgers, G., Mikolajewicz, U., Gröger, M., Maier-Reimer, E., Vizcaino, M., and Winguth, A.: Dynamics of the terrestrial biosphere, climate and atmospheric CO₂ concentration during interglacials: a comparison between Eemian and Holocene, *Clim. Past*, 2, 205–220, doi:10.5194/cp-2-205-2006, 2006.

Sitch, S., Smith, B., Prentice, I. C., Arneth, A., Bondeau, A., Cramer, W., Kaplan, J. O., Levis, S., Lucht, W., Sykes, M. T., Thonicke, K., and Venevsky, S.: Evaluation of ecosystem dynamics, plant geography and terrestrial carbon cycling in the LPJ dynamic global vegetation model, *Global Change Biol.*, 9, 161–185, 2003.

Stouffer, R. J., Yin, J., Gregory, J. M., Dixon, K. W., Spelman, M. J., Hurlin, W., Weaver, A. J., Eby, M., Flato, G. M., Hasumi, H., Hu, A., Jungclaus, J. H., Kamenkovich, I. V., Levermann, A., Montoya, M., Murakami, S., Nawrath, S., Oka, A., Peltier, W. R., Robitaille, D. Y., Sokolov, A., Vettoretti, G., and Weber, S. L.: Investigating the causes of the response of the thermohaline circulation to past and future climate changes, *J. Climate*, 19, 1365–1387, 2006.

Turney, C. S. M., Kershaw, A. P., Lowe, J. J., van der Kaars, S., Johnston, R., Rule, S., Moss, P., Radke, L., Tibby, J., McGlone, M. S., Wilmshurst, J., Vandergoes, M., Fitzsimons, S., Bryant, C., James, S., Branch, N. P., Cowley, J., Kalin, R. M., Ogle, N., Jacobsen, G., and Fifield, L. K.: Climate variability in the Southwest Pacific during the last termination (20–10 kyr BP), *Quaternary Sci. Rev.*, 25, 886–903, 2006.

Van der Kaars, W. A.: Palynology of Eastern Indonesian marine piston-cores: A Late Quaternary vegetational and climatic record for Australia, *Palaeogeogr. Palaeoclimatol.*, 85, 239–302, 1991.

Van der Kaars, S., Penny, D., Tibby, J., Fluin, J., Dam, R. A. C., and Suparan, P.: Late Quaternary palaeoecology, palynology and palaeolimnology of tropical lowland swamp: Rawa Danau, West-Java, Indonesia, *Palaeogeography, Palaeoclimatology, Palaeoecology*, 171, 185–212, 2001.

Vincens, A., Garcin, Y., and Buchet, G.: Influence of rainfall seasonality on African lowland vegetation during the late quaternary: pollen evidence from Lake Masoko, Tanzania, *J. Biogeogr.*, 34, 1274–1288, 2007.

Weaver, A. J., Eby, M., Wiebe, E. C., Bitz, C. M., Duffy, P. B., Ewen, T. L., Fanning, A. F., Holland, M. M., MacFadyen, A., Matthews, H. D., Meissner, K. J., Saenko, O., Schmittner, A., Wang, H., and Yoshimori, M.: The UVic Earth System Climate Model: model description, climatology, and applications to past, present and future climates, *Atmos. Ocean*, 39, 361–428, 2001.

Yeager, S. G., Shields, C. A., Large, W. G., and Hack, J. J.: The low-resolution CCSM3, *J. Climate*, 19, 2545–2566, doi:10.1175/JCLI3744.1,

Zhou, H., Zhao, J., Feng, Y., Gagan, M. K., Zhou, G., and Yan, J.: Distinct climate change synchronous with Heinrich event one, recorded by stable oxygen and carbon isotopic compositions in stalagmites from China, *Quaternary Res.*, 69, 306–315, doi:10.1016/j.yqres.2007.11.001, 2007.

CPD

8, 5359–5387, 2012

Tropical vegetation response to Heinrich Event 1

D. Handiani et al.

Title Page

Abstract

Introduction

Conclusions

References

Tables

Figures

◀

▶

◀

▶

Back

Close

Full Screen / Esc

Printer-friendly Version

Interactive Discussion



Tropical vegetation response to Heinrich Event 1

D. Handiani et al.

Table 1. The original PFTs as simulated by the UVic ESCM and CCSM3 are combined into four main types of PFTs to simplify the model intercomparison (Bonan et al., 2006). The UVic ESCM classification also makes use of the lowest temperature criteria (e.g. Kaplan et al., 2003; Sitch et al., 2003).

PFT description		Broadleaf Evergreen trees	Needleleaf Evergreen trees	Deciduous trees	Grasses
UVic	Broadleaf tree (BL)	X		X	
		IF $T_{c_{min}} \geq 15.5^{\circ}\text{C}$		IF $T_{c_{min}} < 15.5^{\circ}\text{C}$	
ESCM	Needleleaf tree (NL)		X	X	
			IF $T_{c_{min}} \geq -2^{\circ}\text{C}$	IF $T_{c_{min}} < -2^{\circ}\text{C}$	
	C_3 grass (C_3)				X
	C_4 grass (C_4)				X
	Shrubs (SH)				X
CCSM3	Tropical broadleaf evergreen tree	X			
	Tropical broadleaf deciduous tree			X	
	Temperate broadleaf evergreen tree	X			
	Temperate needleleaf evergreen tree		X		
	Temperate broadleaf deciduous tree			X	
	Boreal needleleaf evergreen tree		X		
	Boreal deciduous			X	
	C_4 grass				X
	C_3 grass				X
	C_3 Arctic grass				X

Title Page

Abstract

Introduction

Conclusions

References

Tables

Figures

◀

▶

◀

▶

Back

Close

Full Screen / Esc

Printer-friendly Version

Interactive Discussion



Tropical vegetation response to Heinrich Event 1

D. Handiani et al.

Title Page

Abstract

Introduction

Conclusions

References

Tables

Figures

◀

▶

◀

▶

Back

Close

Full Screen / Esc

Printer-friendly Version

Interactive Discussion



Table 2a. Distribution of dominant PFTs which is based on the percentage of PFT coverage for the UVic ESCM results simulation.

Dominant PFTs or PFTs mixture	PFT coverage
	BL, NL, SH, C ₃ , C ₄ over 50 %
Broadleaf tree (BL)	BL ≥ 50 %
Needleleaf tree (NL)	NL ≥ 50 %
Shrubs (SH)	SH ≥ 50 %
C ₃ grass (C ₃)	C ₃ ≥ 50 %
C ₄ grass (C ₄)	C ₄ ≥ 50 %
	BL, NL, SH, C ₃ , C ₄ less than 50 %
Mixed trees	BL+NL ≥ 50 %
Mixed vegetation (without trees)	SH+C ₃ +C ₄ ≥ 50 %
Open vegetation	20 % ≤ BL+NL+SH+C ₃ +C ₄ ≤ 50 %
Barren soil	BL+NL+SH+C ₃ +C ₄ < 20 %

If the percentage is over 50 %, the PFT potential is set equal to the dominant PFT (broadleaf tree, needleleaf tree, shrubs, C₃ grass, or C₄ grass). If it is less than 50 %, the grid cell is designated as mixed trees if it is dominated by tree PFTs, as mixed vegetation if non-trees PFTs are dominant, as open vegetation if all PFTs are between 20 and 50 % and as desert if all PFTs together are less than 20 % (Crucifix et al., 2005).

Tropical vegetation response to Heinrich Event 1

D. Handiani et al.

Table 2b. The combination of environmental constraints and potential PFTs are used to compute the biome distribution from UVic ESCM results (Handiani et al., 2012).

Dominant PFTs or PFTs mixture	Environmental Constraints					Mega biomes
	Tc min (°C)	GDD5 min	GDD0 min	Tw (°C) min max		
BL tree	15.5					Tropical forest
BL tree or mixed trees	5					Warm temperate forest
BL tree or NL tree or mixed trees	–2					Temperate forest
BL tree or NL tree or mixed trees	–32.5					Boreal forest
Grass (C ₃ , C ₄) or mixed vegetation or open vegetation	17					Savannah and dry woodland
Grass (C ₃ , C ₄) or mixed vegetation or open vegetation		500		10		Grassland and dry shrubland
Barren soil				22		Desert
SH or mixed vegetation					15	Dry tundra
SH or mixed vegetation			800		15	Tundra

The environmental constraints were chosen based on the definition of biomes in the BIOME 4 model (Kaplan et al., 2003).

[Title Page](#)
[Abstract](#)
[Introduction](#)
[Conclusions](#)
[References](#)
[Tables](#)
[Figures](#)
[Back](#)
[Close](#)
[Full Screen / Esc](#)
[Printer-friendly Version](#)
[Interactive Discussion](#)


Tropical vegetation response to Heinrich Event 1

D. Handiani et al.

Title Page

Abstract Introduction

Conclusions References

Tables Figures

◀ ▶

◀ ▶

Back Close

Full Screen / Esc

Printer-friendly Version

Interactive Discussion

Table 3. The biome distribution estimation scheme adopted from a study by Schurgers et al. (2006) applied to the CCSM3 output. The temperature limitation is based on bioclimatic parameters for survival and establishment of PFTs in the CCSM3 (Bonan et al., 2003). The high latitude biome distribution is only classified by Tundra.

PFT fraction (%)		Temperature limitation (°C)	Mega biomes and non-biomes description
$C_v > 20$	$C_f > 80$	$C_{ftrop} > C_{ftemp}$ $C_{ftrop} > C_{fbor}$ $C_{ftemp} > C_{ftrop}$ $C_{ftemp} \geq C_{fbor}$ $C_{fbor} > C_{ftrop}$ $C_{fbor} \geq C_{ftemp}$	Tropical forest Warm temperate forest Temperate forest Boreal forest
		$C_{v,C4} \geq C_{v,C3}$ $C_{v,C3} \geq C_{v,C4}$	$T_c > -17.0$ $T_c \leq -17.0$
$C_v \leq 20$	$C_f \leq 80$	$T_c > 0.0$ $T_c < 0.0$	Desert Ice Barren

C_f forest fraction (sum of cover of all tree PFTs);
 C_{ftrop} tropical forest fraction (sum of cover of all tropical tree PFTs);
 C_{ftemp} temperate forest fraction;
 C_{fbor} boreal forest fraction;
 C_v vegetation fraction (sum of cover of all PFTs);
 T_c air surface temperature;
 $C_{v,C3}$ C_3 grasses fraction;
 $C_{v,C4}$ C_4 grasses fraction.



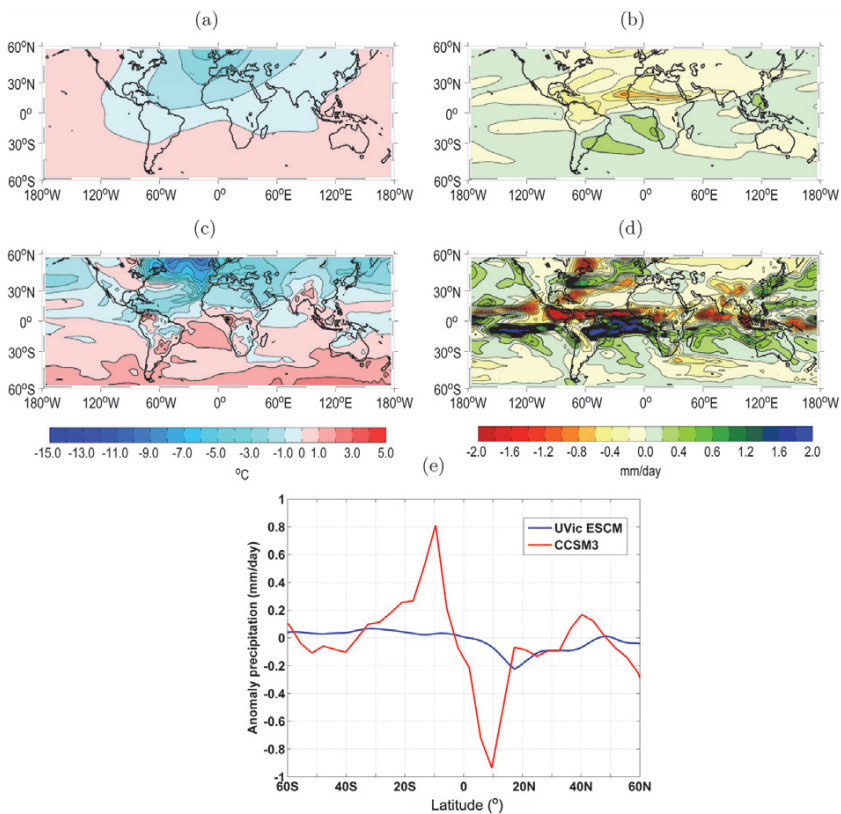


Fig. 1. Annual mean anomalies of surface temperature (**a, c**) and precipitation (**b, d**) between HE1_UVic and LGM_ UVic (top) and between HE1_CCSM and LGM_CCSM (middle) simulations. The contour intervals are fixed at 1°C for surface temperature and 0.5 mm day^{-1} for precipitation. (**e**) The global zonally averaged precipitation differences between HE1 and LGM simulations for the UVic ESCM (blue) and the CCSM3 (red) model.

Tropical vegetation response to Heinrich Event 1

D. Handiani et al.

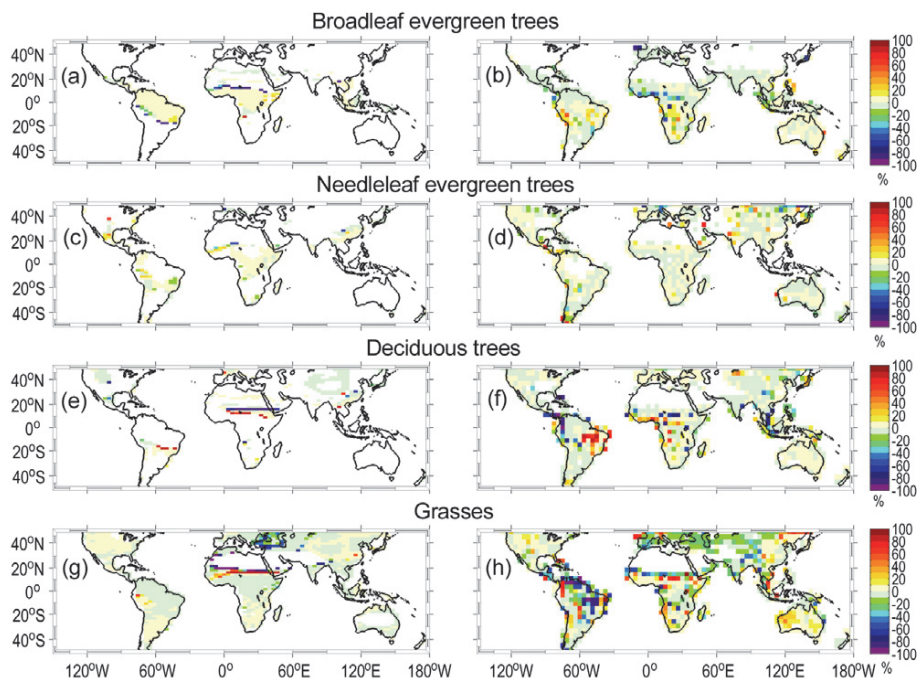


Fig. 2. Annual mean differences of PFT cover between HE1 and LGM simulations for the UVic ESCM (left panels) and the CCSM3 (right panels). The classification into the four PFTs is defined in Table 1.

Title Page

Abstract

Introduction

Conclusions

References

Tables

Figures

◀

▶

◀

▶

Back

Close

Full Screen / Esc

Printer-friendly Version

Interactive Discussion



Tropical vegetation response to Heinrich Event 1

D. Handiani et al.

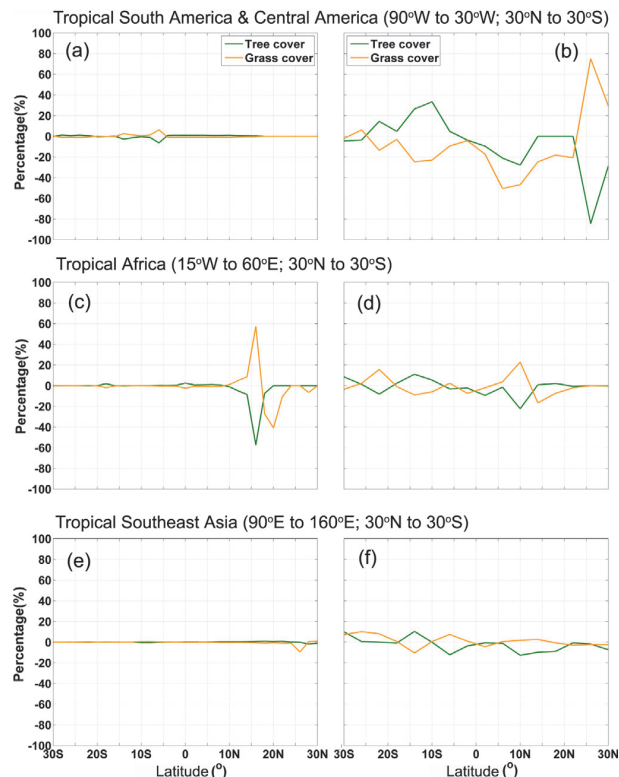


Fig. 3. Annual mean anomalies of regional zonally averaged tree and grass cover between HE1 and LGM for the UVic ESCM (left panels) and the CCSM3 (right panels). The regional areas are tropical South America and Central America (top), tropical Africa (middle) and tropical Southeast Asia (bottom).

Title Page

Abstract

Introduction

Conclusions

References

Tables

Figures

◀

▶

◀

▶

Back

Close

Full Screen / Esc

Printer-friendly Version

Interactive Discussion



Tropical vegetation response to Heinrich Event 1

D. Handiani et al.

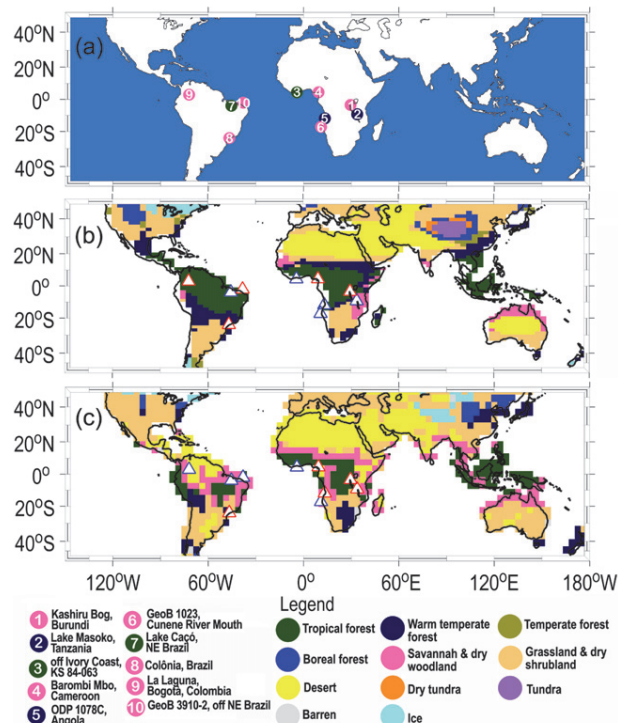


Fig. 4. Sites of HE1 pollen records compiled by Hessler et al. (2010) and the biome reconstruction of each site as represented by the colour of the circle (a, see legend biome distribution). The biome distribution computed from the HE1_UVic simulation (b) and the HE1_CCSM simulation (c) are shown. A comparison between model output and biome reconstruction of each location is indicated by white-blue triangles where biomes are similar in both the model and the reconstruction; white-red triangles denote where modelled and reconstructed biomes differ.